Zhen, Dong, Zhao, H.L., Gu, Fengshou and Ball, Andrew

Phase-compensation-based dynamic time warping for fault diagnosis using the motor current signal

Phase Compensation Based Dynamic Time Warping for Fault Diagnosis Using Motor Current Signal

D. Zhen[1], H. L. Zhao[2], F. Gu[1], and A. D. Ball[1]

[1]Centre for Diagnostic Engineering, University of Huddersfield, HD1 3DH, U.K

[2]College of Information and Electrical Engineering, Shan Dong University of Science and Technology, Qingdao, Shandong, 266510, P.R China

D.Zhen@hud.ac.uk

Abstract. Dynamic Time Warping (DTW) is a time domain based method and widely used in various similar recognition and data mining applications. This paper presents a phase compensation based DTW to process the motor current signals for detecting and quantifying various faults in a two-stage reciprocating compressor under different operating conditions. DTW is an effective method to align up two signals for dissimilarity analysis. However, it has drawbacks such as singularities and high computational demands that limit its application in processing motor current signals for obtaining modulation characteristics accurately in diagnosing compressor faults. Therefore, a phase compensation approach is developed to reduce the singularity effect and a sliding window is designed to improve computing efficiency. Based on the proposed method, the motor current signals measured from the compressor induced with different common faults are analysed for fault diagnosis. Results show that residual signal analysis using the phase compensation based DTW allows the fault related sideband features to be resolved more accurately for obtaining reliable fault detection and diagnosis. It provides an effective and easy approach to the analysis of motor current signals for better diagnosis in the time domain in comparison with conventional Fourier Transform based methods.

Keywords: Reciprocating Compressor, Dynamic Time Warping, Motor Current Signal, Phase Compensation

1. Introduction

Electrical motor current signals have been widely investigated to analyse the health of the induction machine [1, 2]. The influence of mechanical problems that result in rotor disturbances [1] and the presence of load imbalance [3] can be detected through analysing the induction machine stator current signals. Moreover, recent studies [4] have shown that the supply currents can contain components related to abnormalities in downstream equipment such as compressors, pumps, rolling mills, mixers, crushers, fans, blowers and material conveyors, showing that the electrical current based method can be used for diagnosing a wide range of machines. Moreover, it has the merits of remote implementation compared with the main stream vibration method.

However, the key technique used for current signal analysis is based on Fourier Transform (FT) to extract weak fault sideband contents from signals predominated with a supply frequency component and its higher order harmonics. Although it produces satisfactory results, the FT-based method is subject to a number of generic limitations: aliasing, spectral leakage and picket-fence effect. In particular, the latter two factors which often lead to large errors in spectrum estimation so that the weak signature due to faults cannot be resolved properly for accurate fault detection and diagnosis. Although many methods have been developed to improve the limitations of the FT based methods, it never eliminated these completely. In addition, the computation complexity is high which limits its application in real-time condition monitoring.

Thus it seems that techniques based entirely on the time domain signals can avoid the shortcomings of the frequency analysis. In fact, time domain based methods, especially time synchronous average (TSA) [5], have received intensive investigation in recent years for monitoring rotating machines and gained many successful applications. However, a shaft mark signal from an additional channel is needed in implementing TSA based monitoring, which leads to increased cost to applications. Moreover, the common task with time series data is comparing one with another in order to detect the differences between them for further analysis in most applications, such as signature matching [6], speech recognition [7] and condition monitoring [8]. However, the case is often that the two time series in the time domain have similar overall component shapes, but out of synchronization [9] as shown in Figure 1(a). Dynamic Time Warping is a method for aligning such two time series efficiently. The fundamental principle behind DTW is to stretch or compress two time series in order to make one resemble the other as much as possible. DTW finds an optimal warping path between the two time series by using dynamic programming to calculate the minimal cumulative distance. Figure 1(b) shows the alignment of two time series processed by DTW.

The DTW has been acknowledged as a valuable algorithm applied in many areas. Bellman, R. and Kalaba, R. first introduced it on adaptive control processes [10]. Then it has been popularized in the application of word and speed recognition [7, 11-13], electro-cardiogram analysis [14-16], clustering of gene expression profiles [17, 18], biometrics [19, 20], process monitoring [21], and data mining and time series clustering [7, 22]. Recently, Zhen, D. et al have explored it in processing signals from motors for condition monitoring and shown promising results in that the aligned signals by DTW do not lose information and is suitable for fault diagnosis. DTW can also be used to suppress the supply frequency contents and highlight the sideband contents [8, 23]. However, although the DTW has been successfully used in many areas, the singularities effect and calculation time are the main limitations in the real application of DTW. Keogh, E. and Pazzani, M. [9] introduced the “singularities” behaviour in the application of DTW, which can lead to inaccurate alignments where a single point on one time series maps onto a large subsection of another time series. In addition, if the length of the two time series is N and M respectively, the accumulated distance matrix will have N×M entries, and then the time complexity will be 0(NM) [24, 29]. This will be especially problematic for embedded systems that have limited resources. In the study of proposed approach, phase estimation and compensation techniques are used to improve the singularities effect of DTW and a sliding window is designed to process the time series using DTW in frame in order to improve the time complexity of DTW calculation for its real-time application.

The rest of the paper will be organized as follows. In section 2, the singularity effect of DTW is studied to identify its influence on signal alignment. Section 3 introduces the phase compensation method to reduce the singularities effect and highlight the reliability and accuracy of DTW algorithm for dissimilarity recognition. The proposed method for feature extraction based on DTW is detailed in section 4. Section 5 presents the evaluation results using the proposed method. Finally, we discuss related issues and conclude in section 6.

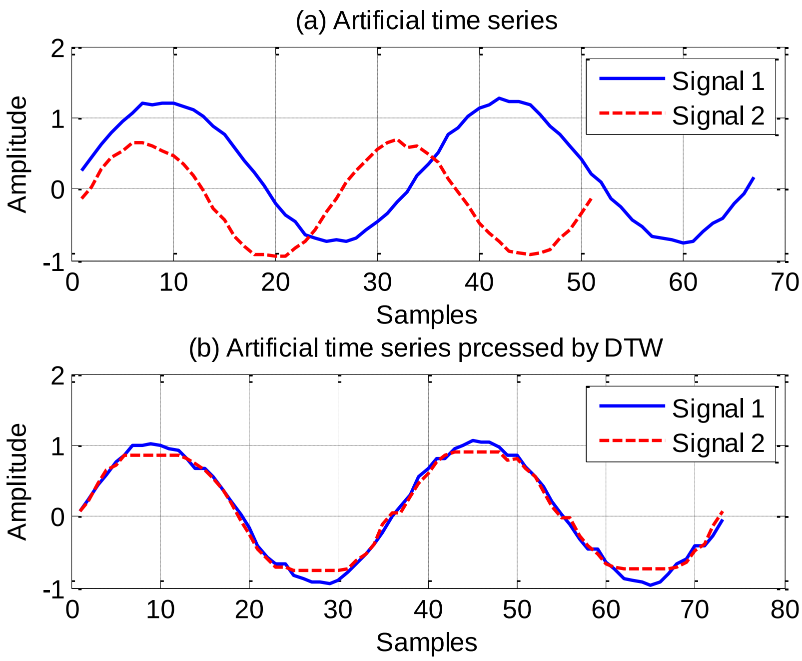

Figure 1 Time series aligned by DTW

2. Dynamic Time Warping Singularities

DTW is an effective algorithm for measuring dissimilarity between time series and has been widely used in various applications. However, DTW warps the X-axis based on the values variability in the Y-axis and the difference between the two points from the two time series is minimal in terms of values. This comparison of values makes the DTW ignore the trend of the points for local accelerations and decelerations in the whole time series. In other words, DTW algorithm only considers the Y-axis value of a data point, but does not consider its local and global features. Therefore, an undesirable alignment where a single point on the one time series maps onto a large subsection of another time series will take place during the processing of DTW. This undesirable alignment is called ‘singularities’ which is proposed by Eamonn and Michael [9]. DTW may fail to align a pair of sequences on their common trends or patterns due to singularity effects, especially when singularities appear at the ends of the aligned time series. Figure 2 illustrates typical singularities located at samples of 8, 20, 32 and 45 in signal 2 where one point on signal 2 maps on numerous points on signal 1.

Various improvements have been proposed to process the singularities and hence to enhance the accuracy of DTW alignment. Keogh et al [9] developed Derivative Dynamic Time Warping (DDTW) which has the ability of not only considering the Y-axis of the data points, but also considering the higher level feature of local feature. DDTW estimates the first derivative of the aligned time series and replaces the value of each data point with its estimated first derivative which can be considered as a local feature of the data point that expresses the relationship with two adjacent neighbours. The estimation of the first derivative of a data point is the average of the data point and its left and right neighbour points. It is more robust to outliers than any estimate considering only two data points for the comparison. Moreover, DDTW considers the square of the difference of the estimated derivatives as the point-to-point distance instead of the Euclidean distance which is used in DTW. However, global features, in other words, the overall shapes or significant features that take place in the whole time series, may be unable to follow in DDTW. With the purpose of capture trends or local and global features of a time series during the alignment process, Ying Xie and Bryan Wiltgen [25] developed a Feature Based Dynamic Time Warping (FBDTW) method to align two time series based on the local and global features of each data point and the improvement of singularities is obvious. Moreover, many other methods have also been proposed to improve the singularities, such as windowing [13], slope weighting [6, 12], and step patterns [6, 13]. All these methods may moderate the effects of singularities, but the improvement is limited when the singularities occurred at the starting or ending of the aligned time series which can lead to larger distortion and cause inaccurate alignment.

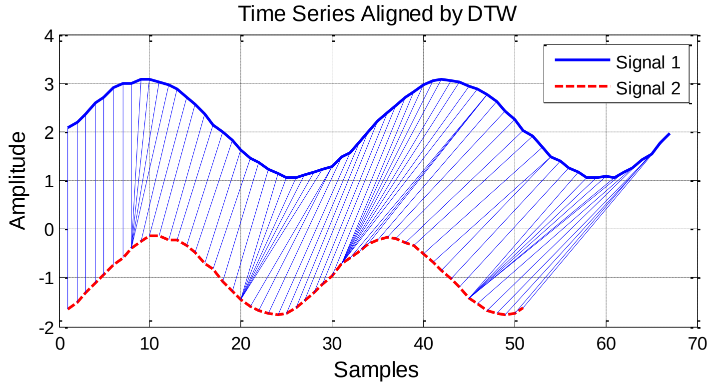

Figure 2 Example of singularities in DTW application

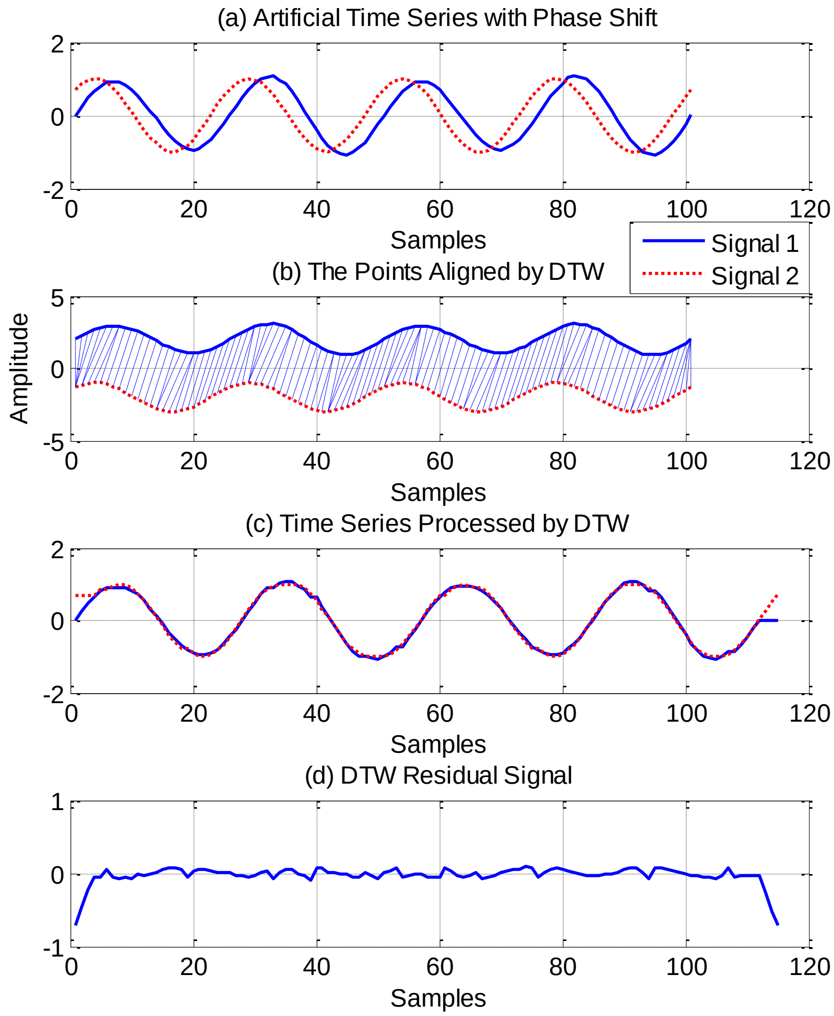

Figure 3 Singularities located in the ends

Figure 3 gives an example of singularities located at the ends of the aligned time series during the DTW procedure. In Figure 3(a), signal 1 is an amplitude modulated signal while signal 2 is a pure sinusoidal signal. The frequency of the carrier signal of signal 1 is the same with the frequency of signal 2, but the two signals have different initial phases and amplitudes. The two signals are aligned by DTW and the point alignments are shown in Figure 3(b), which indicates the singularities during the DTW processing, especially at the ends of the signals. From Figure 3(c), it can be seen that the alignment is poor at the starting and ending of the time series, which can lead to inaccurate dissimilarity estimation. The residual signal comparing the two time series is shown in Figure 3(d). It is clear that the residual signal is unreliable due to the data jump in the ends caused by singularities during DTW procedure. The singularities located in the ends may be due to the phase shift based on analysing the DTW processing shown in Figure 3.

According to the definition of DTW in [9, 22], the optimal warping path is selected through finding the minimal distance in the accumulated distance matrix which is built based on the distance matrix. The elements of the distance matrix are the point-to-point Euclidean distance between the two time series. If there is a phase shift between the two time series, the Euclidean distance between the first points of the two time series is not the minimal in the first column or row of the distance matrix. Therefore, the distribution of the accumulated distance matrix is changed accordingly and hence the optimal warping path selected according to step patterns [6] could not approached to the diagonal of the accumulated distance matrix as much as anticipated. Moreover, the accumulated error of the accumulated distance matrix will be increased due to the increased values in the distance matrix caused by the phase shift between the two time series. The accumulated error leads to inaccurate minimal distance findings in the dynamic programming of DTW and hence more warping jumps will occur, especially at the starting and ending of the aligned time series due to the first or last point on one time series maps onto numerous points on the other time series, as shown in Figure 3(b), which causes the singularities.

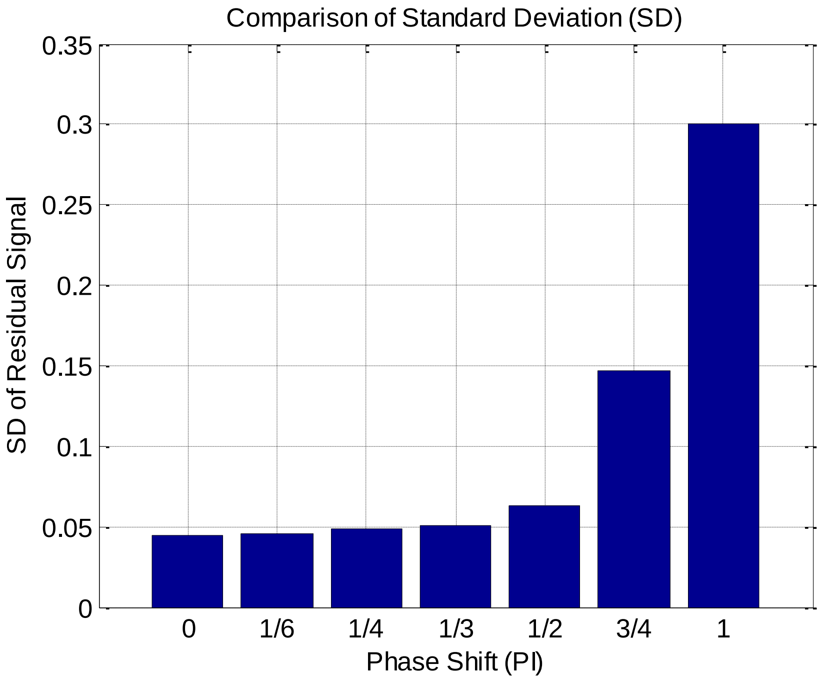

Figure 4 SD of DTW residual signals with different phase shifts

To study the impact of phase shift on singularities, different phase shifts θ_i from 0 to π between the two time series are explored. Figure 4 shows the standard deviation (SD) of the DTW residual signals from different pairs of time series of different phase shifts. The phase shift is 0 denotes the two aligned signals which have the same initial phase, whereas π means an opposite phase between two signals. It reveals that with the increase of the phase shift, the SD value of DTW residual signal is increased clearly, demonstrating that larger phase shift leads to larger accumulated error in accumulated distance matrix and greater data jumps in the residual signal. This shows that DTW produces different dissimilarity results at different phase shifts even if the two signatures in comparison are the same.

This will lead to uncertainty of fault diagnosis when comparing measured signals with different phases due to different acquisition time instants.

3. Phase Compensation Based Dynamic Time Warping

To verify the ability of phase compensation in the singularity effects improvement, phase estimation and compensation are carried out on the two time series before DTW is implemented. An initial phase needs to be estimated for a preliminary alignment between the two aligned time series. In the proposed method, the initial phase estimation is developed by a phase matching approach. Assuming that two time series with the same length but with different initial phases are expressed in Equation (1) and shown in Figure 3(a),

$$s_1 = \{s_{11}, s_{12}, \cdots, s_{1i}, \cdots s_{1n}\}\ and\ s_2 = \{s_{21}, s_{22}, \cdots, s_{2i}, \cdots s_{2n}\} \tag{1}$$

In the initial phase estimation, the Euclidean distance given by Equation (2) is used to measure the differences between the two time series at different phases θ. As the phase θ varies from 0 to 2π in a step of $\pi/180$, thus, the Euclidean distances of the two time series can be obtained.

$$D_j = \sqrt{\sum_{i=0}^{n}\left[s_{1i} - s_{2i}(\theta_j)\right]^2}\ where\ j = 1,2,\cdots,N \tag{2}$$

where, s_{1i} indicates one time series without phase shift, and $s_{2i}(\theta_j)$ denotes another time series with a certain phase shift of θ_j, and n is the number of points in the time series. D should have N elements according to the increase of the phase θ, where N is the number of changes of θ. Therefore, each phase angle θ_j should correspond to one Euclidean distance D_j in the matrix D. The initial phase shift can be obtained by finding the phase angle θ_e which corresponds to the minimal Euclidean distance in the matrix D.

$$D = \{D_1, D_2, \cdots, D_j, \cdots, D_N\}\ \text{Subject to}\ \theta = \{\theta_1, \theta_2, \cdots, \theta_j, \cdots \theta_N\} \tag{3}$$

$$[D_{min}, \theta_e] = Min(D) \tag{4}$$

Thus the phase of the time series s_2 can be compensated using the estimated phase angle θ_e to obtain minimal initial phase shaft compared with the time series s_1.

Figure 5(a) shows the result of phase estimation and compensation of the two time series which is shown in Figure 3(a). It can be seen that the overall waveform of the two time series are matched better after phase compensation. From the processing results of DTW shown in Figure 5(b) and (c) and DTW residual signal shown in Figure 5(d), it is clear that the singularities at the ends of the aligned time series as shown in Figure 3(b) are moved out and this proves that phase compensation is able to improve the singularity effects of DTW and reduce the data jumps at the ends of DTW residual signal. Therefore, more accurate results of dissimilarity recognition by DTW can be obtained after processing by phase compensation.

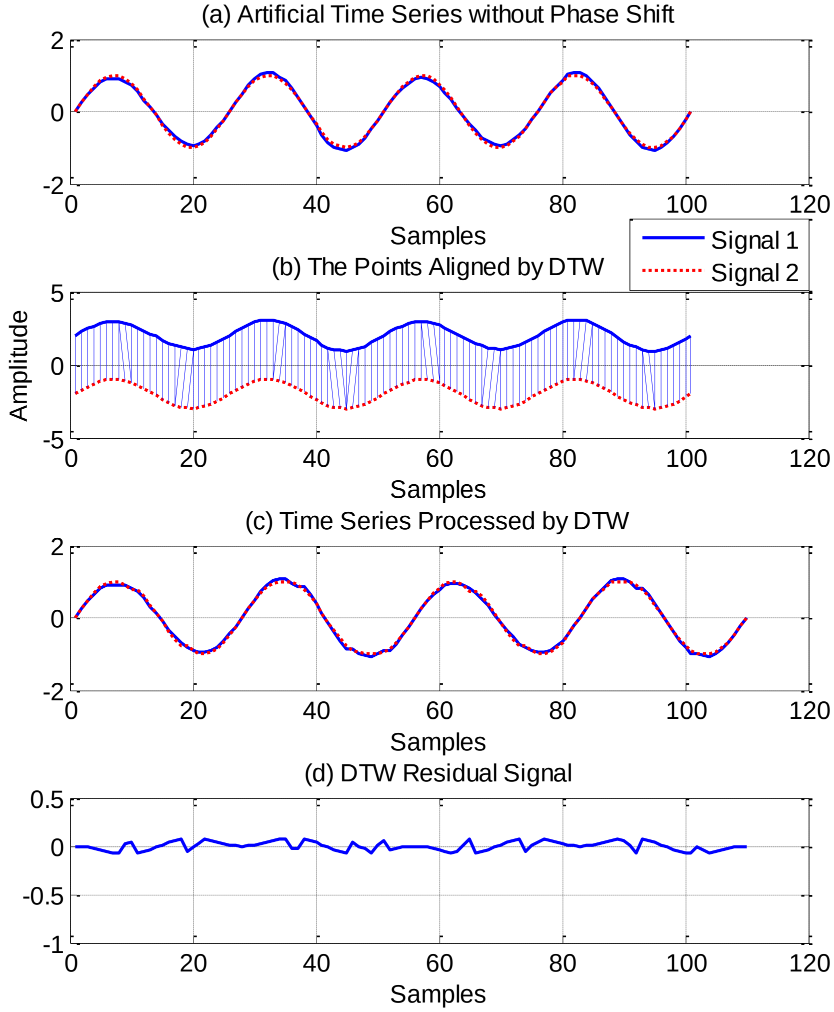

Figure 5 Singularity effect of DTW with phase compensation

Figure 6 shows the comparison of SD values between phase compensation and non-compensation. It can be seen that without phase compensation, the SD values increase with the phase shifts between the two time series. However, the SD values of DTW residual signals obtained from the two time series after phase compensation are all similar. This means that the phase compensation can reduce the effect of singularities to maintain the minimal value of dissimilarity between the two signals of different phase shifts, which in turn allows accurate feature extraction for obtaining reliable fault detection and diagnosis.

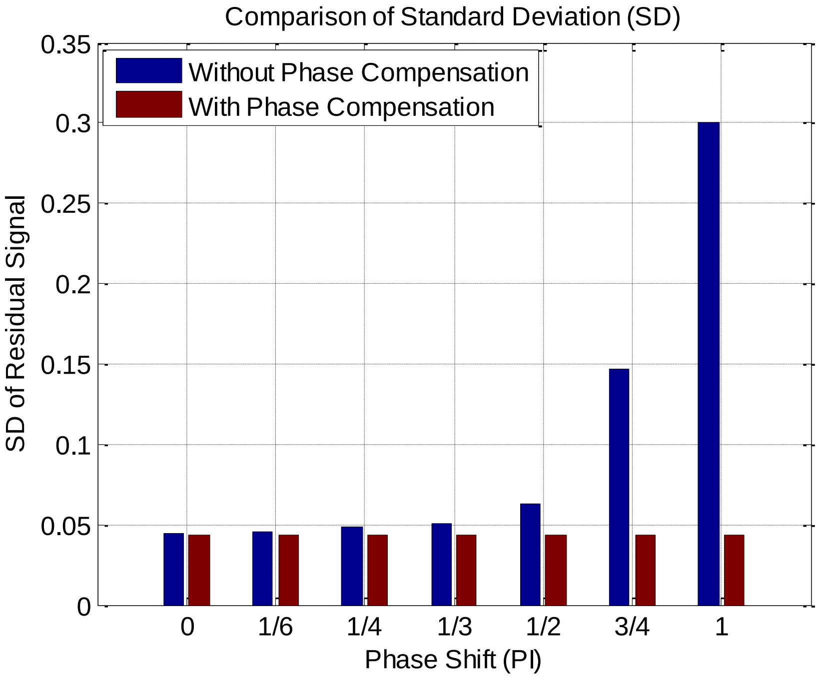

Figure 6 Comparison of SD of DTW residual signals

4. Feature Extraction of Motor Current

In order to extract the features of motor current signal for fault detection and diagnosis, the characteristics of the current signal need to be analysed appropriately. Moreover, effective data processing procedures based on DTW should be premeditated to obtain accurate feature extraction results.

4.1 Motor Current Signal

The electrical current signal is a typical amplitude modulation (AM) signal [4]. A reciprocating compressor system consists of an induction motor, in which the compressor has two basic working processes including compression and expansion. The working process gives rise to a periodically varying load to the driving motor due to the compressor requiring more power in compression than in expansion [26]. This varying load leads to high oscillation in the measured current signal. Figure 7 shows the motor current signals measured from a two-stage reciprocating compressor under the conditions of healthy and faulty valve leakage. From the waveform of the current signal shown in Figure 7(a), it can be seen that the amplitude of the current waveform from the valve leakage is slightly higher than that of the healthy condition and the current signals are modulated by a dynamic load fluctuating. It is also very clear that the two current signals have similar waveforms but with clear phase shift.

In the spectra, as shown in Figure 7(b), it can be seen that the main frequency contents contained in current signals are the supply frequency which is about 50Hz and the load fluctuating frequency of 7.3Hz which corresponds to the working frequency of the compressor. The carrier frequency components at the supply frequency 50Hz have high amplitudes and the sideband contents at about 50±7.3Hz are also very clear. Nevertheless, the amplitude of the two sideband contents will change with the degree of load and speed fluctuations. The upper sideband content results from the lower sideband content due to a nonlinear effect caused by the interaction of magnetic flux, load and speed fluctuations [27, 28]. Therefore, the motor current signals contain useful information for compressor fault detection.

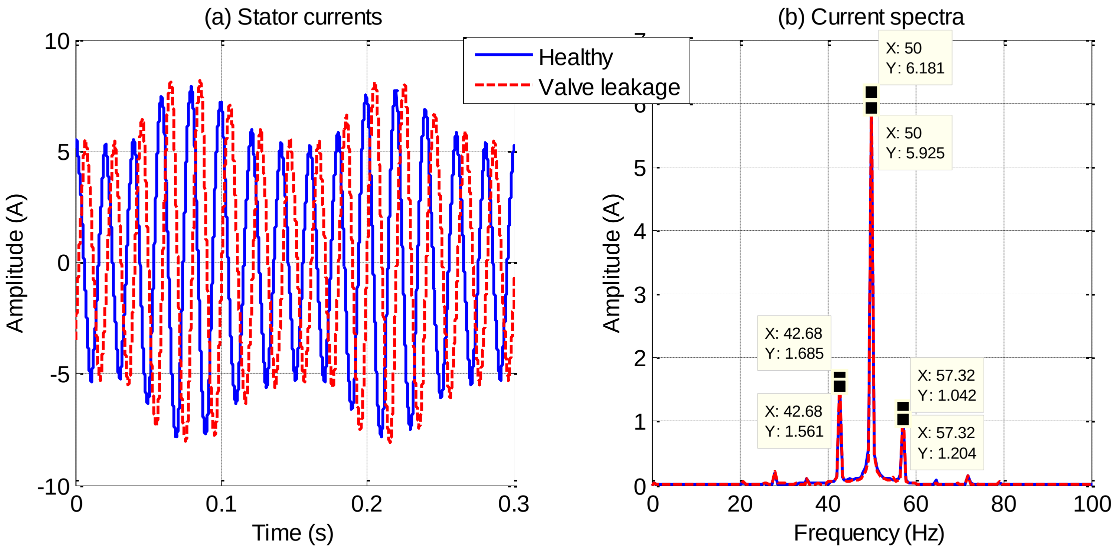

Figure 7 Waveform and spectra of current signals from compressor

However, the components at 50Hz have a clear spectral leakage due to the limitation of FT calculation. This leakage will lead to an error in estimating the amplitude at 50Hz, which causes in turn more difficulties in identifying and quantifying the weak sidebands which are the main features used for compressor fault diagnosis. It means that the features obtained in the frequency domain degrade fault diagnosis performance and a more accurate estimation of the sideband characteristics need to be used.

4.2 Feature Extraction Procedure

To separate the fluctuating component from the supply component as accurately as possible in motor current signals, a DTW approach based on the introduction of a reference signal which has the same frequency contents with the supply power is suggested to apply to the current signals for feature extraction. The approach has the data manipulation steps as follows.

Step1: Data Pre-processing

The purposes of data pre-processing is to suppress the inevitable random noise. It is carried out by a low-pass filter with the cut-off frequency of 120Hz so to remove both the high order harmonics of supply frequency and any random noise originated from measurement and power supply system. This will ensure that the DTW and frequency estimations can be implemented reliably.

Step2: Reference Signal Generation

The reference signal is defined as a sinusoidal signal with the frequency and amplitude calculated from the filtered measured signal. Supposing that the filtered measured signal is $\{x_1, x_2, \cdots, x_n\}$, the amplitude of the reference signal is estimated by

$$A_{ref} = \sqrt{2}\sqrt{\frac{1}{n}\sum_n x_n^2} \tag{5}$$

The frequency is estimated by the zero-across detection method. It finds the zero crossing points in a predetermined time interval and counts the number of cycles m that occur in the time interval to obtain the frequency estimation as

$$f_{ref} = Fs/m \tag{6}$$

where Fs is the sampling frequency. Thus the reference signal can be generated by

$$x_{ref} = A_{ref}cos(2\pi f_{ref}t) \tag{7}$$

Step3: Phase Estimation and Compensation

The initial phase shifts between the measured current signal and reference signal is estimated based on the method proposed in section 3. The estimated phase shift θ_e can be obtained by Equation (4), and hence the reference signal can be regenerated as Equation (8) to have minimal initial phase compared with the filtered measured signal.

$$x_{ref} = A_{ref}cos(2\pi f_{ref}t + \theta_e) \tag{8}$$

Step4: Window Length Determination

A sliding window is designed to improve the computing efficiency of DTW implementation. The estimation of the minimum length of the sliding window for DTW processing can be found by calculating the load fluctuating components which corresponds to the working speed of the compressor.

$$Lmin = Fs/f_c \tag{9}$$

And the load fluctuating components can be calculated,

$$f_c = S/(60R) \tag{10}$$

where S and R are the speed and transmission ratio of the compressor, respectively. The actual length of the sliding window may be several times of the minimal length $Lmin$ depending on data processing tasks. For benchmarking proposed methods with FT based methods, the length of the sliding window is set to 3 times of $Lmin$ so that the FT based results can have a sufficient resolution for sideband features extraction in the frequency domain.

In addition, to align the reference signal and the filtered measured signal, the length of the reference signal should be the same with that of the sliding window for high efficiency in DTW implementation and memory allocation.

Step5: DTW Implementation

After designing the reference signal and determining the length of the sliding window, the DTW algorithm can be applied to process the reference signal and the measured signal selected by frame by frame. The two signals are aligned in the time domain after being processed by DTW, and hence a residual signal can be obtained by subtracting the reference signal by the measured signal and the dissimilarity between the two signals can be shown by the residual signal. The window is sliding along the measured signal. Therefore, the DTW can be implemented efficiently in each sliding window to reveal the differences.

Figure 8 shows the interim results of DTW processing at each key step in a typical sliding window. The measured signal is presented with an initial phase when the data is collected in Figure 8(a) and the reference signal is presented with 0 initial phase. Obviously, these two signals are shifted from each other greatly and cannot be compared directly. Figure 8(b) shows the result after phase compensation on the reference signal through the initial phase matching. It can be seen that the overall waveforms are better matched, but many detailed portions in the waveform are still not matched sufficiently well for comparison. After DTW processing, the measured signal and reference signal are matched to their optimal as shown in Figure 8(c) and hence the dissimilarity can be revealed by subtraction directly. The phase estimation and compensation is a low consumption process, and its time-consuming is only 0.5% of DTW implementation when the sampling frequency is at 24 kHz. Figure 8(d) shows the residual signal obtained by the subtraction. Clearly the residual signal highlights the major differences between the waveforms that are shown in Figure 8(a) which is around the peak portion of the amplitude modulation when the motor has been applied by higher load during the compensation process, which has the higher effects of mechanical process. As a result of this signal enhancement, a more accurate feature can be extracted from this residual signal.

Step6: Feature Detection

The aim of applying DTW to process signal is to recognize the differences between the two signals with higher accuracy, and the residual signal is used to demonstrate the differences. Therefore, the detection can be made through analysing the residual signal. In the proposed method, the RMS values of the residual signal are employed to measure the amplitude of the residual signals. Compared with peak values, the RMS values produce a more reliable feature when the form of AM modulation varies with different operating conditions and fault cases. Obviously, a higher RMS value indicates a greater difference between the reference signal and the measured signal and hence it indicates the deviation degree of the signal from sinusoidal due to the modulation effects under compressor conditions.

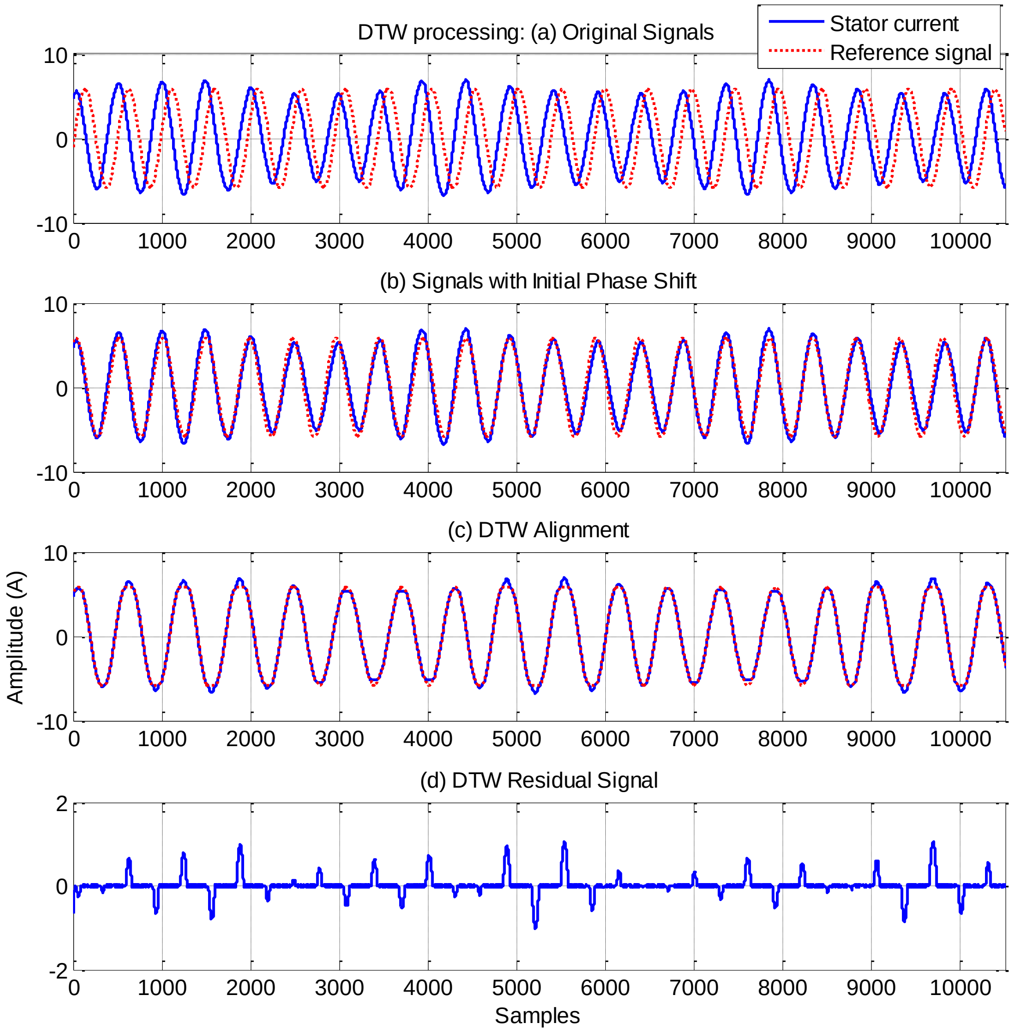

Figure 8 DTW processing motor current signal

5. Experimental Evaluation

To evaluate the performance of the proposed approach in fault detection and diagnosis, electrical current signals are collected from a two-stage reciprocating compressor induced with a number of common faults. The signals are then processed by proposed approach to produce fault detection and diagnosis results. In addition, the results are also compared with that from traditional FT analysis.

5.1 Experimental Tests

The reciprocating compressor has a common two-stage construction which allows air to be compressed as high as 10bar. It is driven by a 2.5kw three-phase four-pole induction motor through a V-belt with a transmission ratio of 3.2. During the tests, the compressor is induced with three comment faults: discharge valve leakage, transmission belt looseness and inter-cooler leakage. These faults can induce low operating efficiency and potential damage to the compressors. The leakage is usually caused by thermal impacts and mechanical vibrations and the belt looseness is a typical feature with the texture of the belt showing some damage. The three types of faults are induced individually to the compressor for evaluating the effectiveness of the proposed method in detecting these faults. The valve leakage is produced by drilling a 1mm hole in the discharge valve plate. The distance between two belt pulleys is reduced by 2mm for belt looseness. The case of inter-cooler leakage is induced by adjusting the tightness of the connecting bolt for the degrees of leakage, which is often a consequence of the resonance of the connection line. In addition, the faults, loads and speeds setting in the experimental process are listed in Table 1, and the experimental setup is shown schematically in Figure 9.

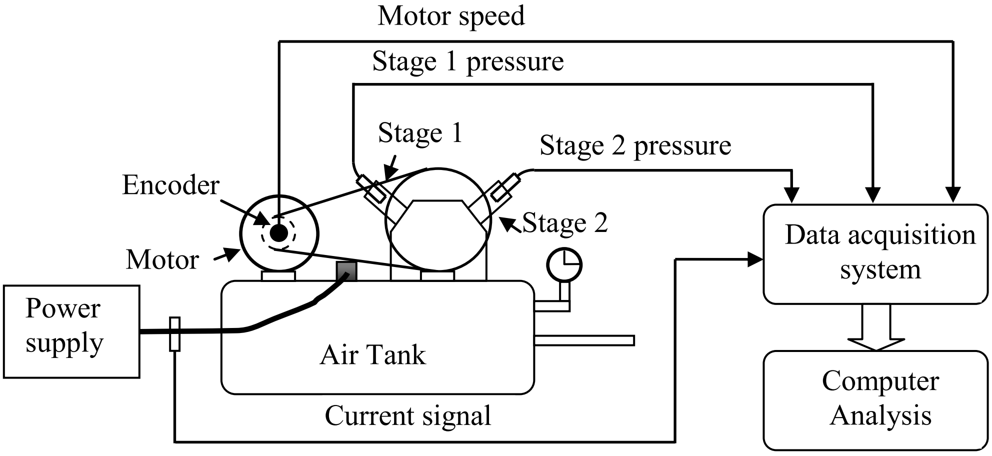

Figure 9 The experimental setup

Table 1 Faults and Loads in using Experimental testing

Conditions	**Load-1 (bar)**	**Load-2 (bar)**	**Load-3 (bar)**	**Load-4 (bar)**	**Load-5 (bar)**	**Load-6 (bar)**	**Nominal Speed (rpm)**
Health	4.8	5.5	6.2	6.9	7.6	8.3	1400
Valve leakage	4.8	5.5	6.2	6.9	7.6	8.3	1400
Inter-cooler leakage	4.8	5.5	6.2	6.9	7.6	8.3	1400
Belt looseness	4.8	5.5	6.2	6.9	7.6	8.3	1400

During the tests, one phase in the three-phase motor current is measured by a Hall effect-based current transducer with frequency response from DC to 1.5 kHz. The current signal is collected by a high speed ADC system at a resolution of 16bit. For each fault the data is collected at 6 different discharge pressures from 4.8bar to 8.3bar, which covers the operating pressure range specified by the manufacturer. Each collection is 50000 points which is more than 2 seconds in duration for a sampling rate of 24.3 kHz. This data length covers about 12 compressor cycles which is sufficient for random noise suppression in an average process. In addition, the high sampling rate allows high accuracy to be obtained in waveform parameter calculation.

5.2 Faults Detection and Diagnosis

The measured current signals are processed by the proposed method to obtain residual signals respective to each case and operating pressures by using the proposed DTW based approach. During the processing, the sliding window is set to 10500 points in length so that it includes about 3 compressor cycles, which allows sufficiently good frequency resolution in FT based analysis in the comparison study. To quantify these differences for separating these fault cases, RMS values of the residual signals are calculated for all cases. Figure 10 shows the RMS values of residual signals from different fault cases at different discharge pressures. It is clear that the RMS values of the residual current signals change with the degree of load oscillation. When the compressor operates at a special discharge pressure, such as 6.2bar, the RMS values of the residual signals are also changing with the different kinds of fault cases. The RMS value of the residual signal under the fault of valve leakage is higher than that of healthy condition and the RMS value of the residual signal under the fault of belt looseness is the lowest in the four fault cases. Moreover, when the discharge pressures increases, the RMS values of the residual signals are increasing accordingly under each kind of fault case. This means that if there is a fault in the compressor, the load fluctuation characteristics will be altered and hence the RMS values and its distinctive will be different from that when the compressor is healthy with the increase of the discharge pressures. Based on this analysis, the faults can be detected by an RMS linear classifier in association with the discharge pressures.

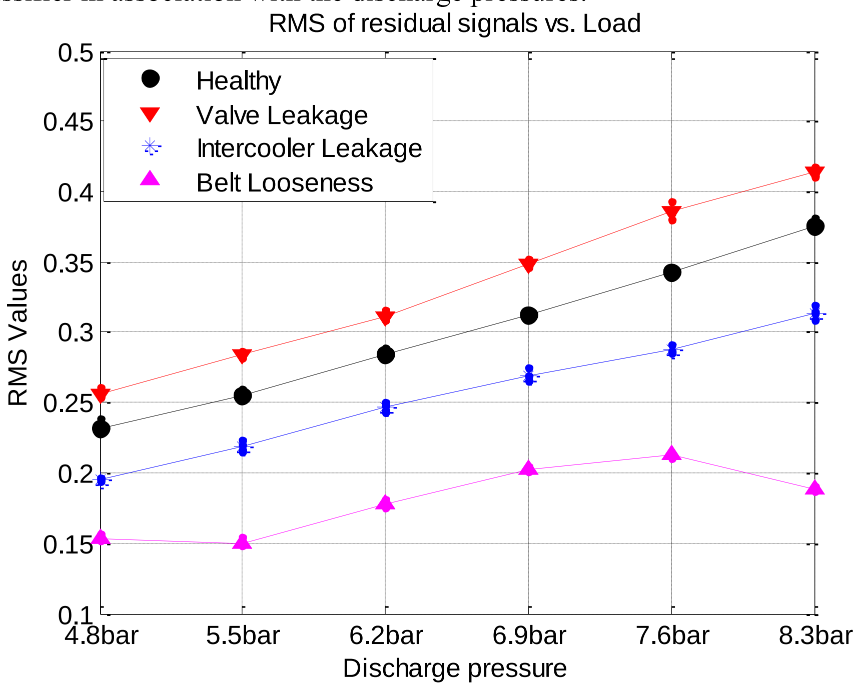

Figure 10 DTW residual signal based detection and diagnosis

5.3 Comparison Conventional Analysis

To benchmark the performance of the proposed method, the modulation characteristics of the current signals are analysed by two conventional methods: FFT based spectrum technique which leads to a sideband amplitude as detection feature and Hilbert transform analysis which produces an envelope level as the detection feature.

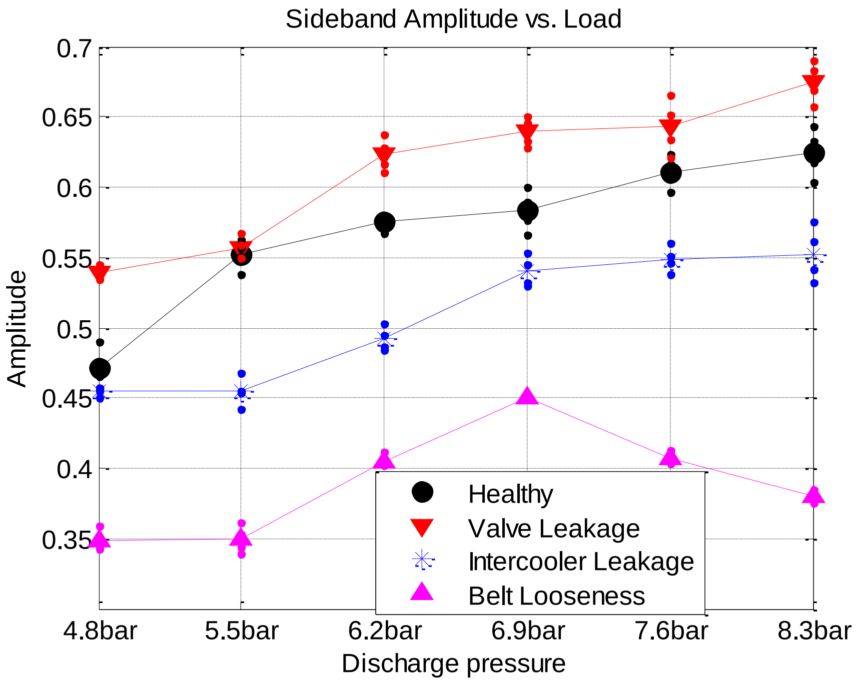

Figure 11 Sidebands from FFT based detection and diagnosis

In performing FFT calculation a hanning window is used to reduce the spectral leakage effects. Figure 11 shows the results from the spectrum analysis technique. The feature extraction is carried out by extracting the spectral peak values of the sideband contents which are used to reveal the differences between different operating conditions. It can be seen that the sideband amplitudes are unable to produce a full separation result between different fault cases under various loads.

In calculating the envelope, a band pass filter with 80Hz bandwidth is applied to the measured current signals and then a FFT based Hilbert transform method is used to obtain the envelope signals. Figure 12 shows the RMS values of envelope signals for different fault cases under the different operating discharge pressures. It shows that the envelope analysis can also allow a full separation between the fault cases under the operating conditions of interest. The overall trend is very similar to the results of the proposed DTW based method, demonstrating that the proposed method is able to capture the modulation characteristics with good accuracy. However, as the RMS values of envelope signals are calculated in the time domain hence spectral leakage etc may be minimised in the time domain envelope signals.

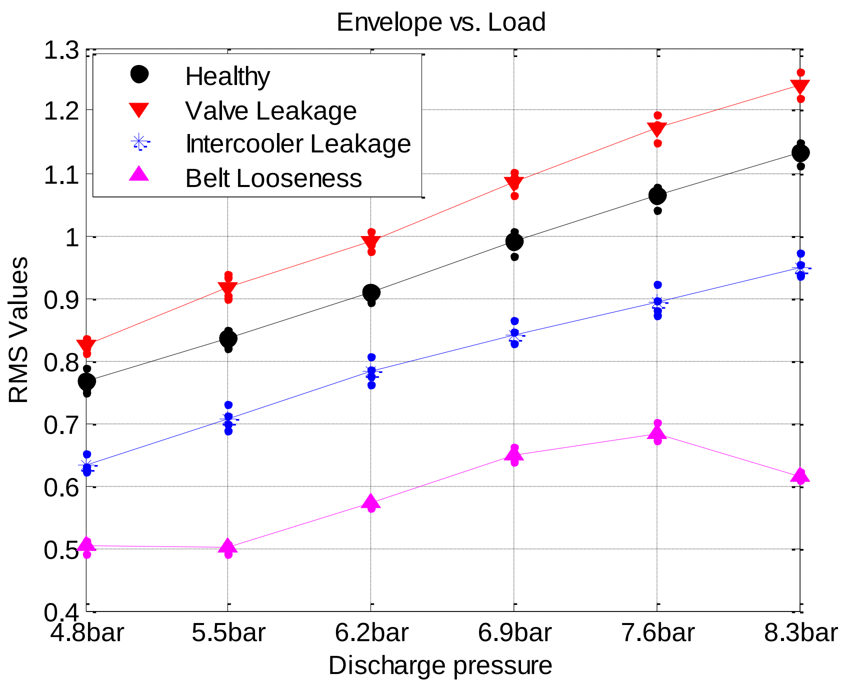

Figure 12 Envelope signal based detection and diagnosis

A careful comparison of the results of the analysis of the proposed method and envelope based analysis also finds that the deviation of RMS values of envelope signal is slightly wider than that of DTW residual signals, where concentrated distribution demonstrates accurate and reliable detection results. Figure 13 shows the relative standard deviation (RSD) for the three methods. It has found that the proposed DTW based method has the smallest deviation among the three analysis techniques, which indicates that the proposed method can produce more reliable diagnostic results.

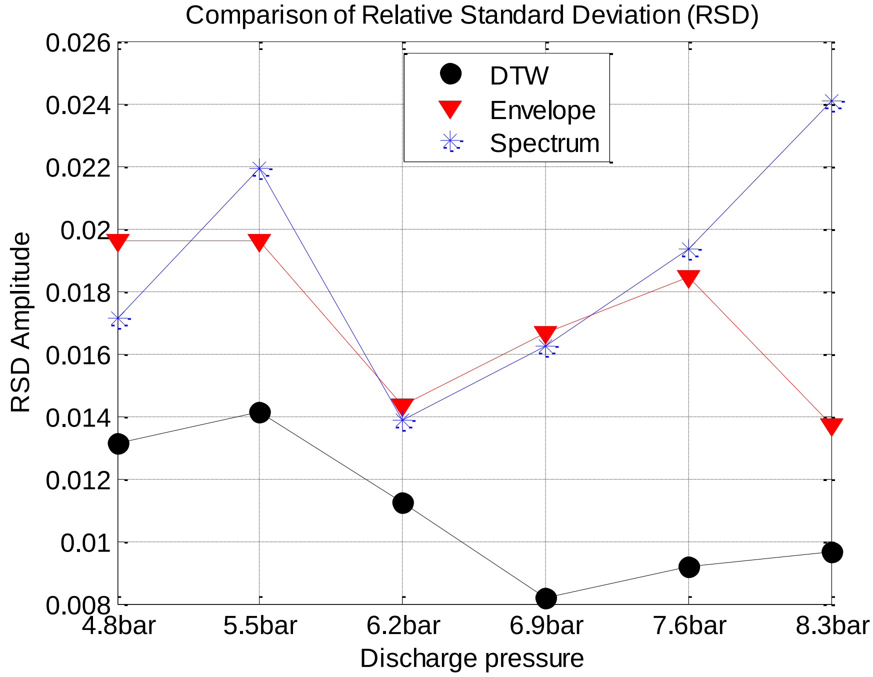

Figure 13 Comparison of standard deviation of three analysis techniques

6. Conclusions

This work shows that the analysis of motor current signals using a phase compensation DTW method has the significant potential to detect and identify the presence of incipient faults in motor drive machines. The initial phase estimation and compensation can improve the singularity effect of DTW and enhance the accuracy and reliability of dissimilarity recognition. The results show that the sideband features or modulation characteristics in current signals can be extracted by DTW through the introduction of a reference signal of the same frequency with the supply power, which leads to a residual signal that contains mainly the sideband contents.

This residual signal is then further analyzed to extract accurate and effective features from the motor current signals measured under different conditions. Based on the analysis, RMS value is developed to classify common compressor faults including valve leakage, intercooler leakage and belt looseness. The analysis results indicate that the phase compensation based DTW method can be employed to extract accurate features of the current signals and RMS values of the residual signals can be used to differentiate the faulty from the healthy and identify the difference between other fault cases under various loads of discharge pressures. Moreover, the accuracy and reliability of detection and classification from phase compensation based DTW analysis is higher than that from FFT spectrum and envelope analysis. In addition, the proposed processing procedure which is based entirely on the time domain analysis is computationally efficient and easier to apply to real-time monitoring.

References

[1] Benbouzid M E H 2000 A Review of Induction Motors Signature Analysis as a Medium for Faults Detection IEEE Transactions on Industrial Electronics, vol.47, no. 5, pp. 984-993

[2] Stack J R, Habetler R G and Harley R G 2004 Bearing fault detection via autoregressive stator current modeling Industry Applications, IEEE Transactions on, vol. 40, no. 3, pp. 740-747

[3] Obaid R R, Habetler T G, Tallam R M 2003 Detecting load unbalance and shaft misalignment using stator current in inverter-driven induction motors Electric Machines and Drives Conference, 2003. IEMDC'03. IEEE International , vol.3, no.1, pp. 1454- 1458

[4] Gu F S, Shao Y M, Naid A and Ball A D 2011 Electrical motor current signal analysis using a

modified bispectrum for fault diagnosis of downstream mechanical equipment Mechanical Systems and Signal Processing, 25 (1), pp. 360-372. ISSN 0888-3270
[5] Dalpiaz G, Rivola A, and Rubini R 2000 Effectiveness and Sensitivity of Vibration Processing Techniques For Local Fault Detection in Gears Mechanical Systems and Signal Processing, vol.14, Issue 3, pp. 387-412, ISSN 0888-3270
[6] Myers C, Rabiner L, and Rosenberg A 1980 Performance tradeoffs in dynamic time warping algorithms for isolated word recognition Acoustics, Speech, and Signal Processing, IEEE Transactions on, vol. 28, no. 6, pp. 623-635
[7] Sakoe H and Chiba S 1978 Dynamic programming algorithm optimization for spoken word recognition Acoustics, Speech and Signal Processing, IEEE Transactions on, vol. 26, no. 1, , pp. 43-49
[8] Zhen D, Gu J, Wang T, Gu F S and Ball A.D 2010 Diagnostic Feature Development based on Dynamic Time Warping of Dynamic Signals under Variable Machine Operating Condition The Seventh International Conference on Condition Monitoring and Machinery Failure Prevention Technologies, 22-24 June 2010, Stratford-upon-Avon, UK.
[9] Keogh E and Pazzani M 2001 Derivative Dynamic Time Warping In Proc. of the First Intl. SIAM Intl. Conf. on Data Mining, Chicago, Illinois
[10] Bellman R and Kalaba R 1959 On adaptive control processes Automatic Control, IRE Transactions on, vol. 4, no. 2, 1959, pp. 1-9
[11] Velichko V M, Zagoruyko N G 1971 Automatic Recognition of 200 Words International Journal of Man-Machine Studies, vol.2, pp. 223-234, 1970.
[12] Sakoe H, Chiba S. 1971 A Dynamic Programming Approach to Continuous Speech Recognition In Proceedings of the Seventh International Congress on Acoustics, vol. 3, pp. 65-69
[13] Itakura F1975 Minimum prediction residual principle applied to speech recognition Acoustics, Speech, and Signal Processing, IEEE Transactions on, vol.23, no.1 pp. 67-72
[14] Huang B, Kinsner W 2002 ECG Frame Classification Using Dynamic Time Warping Electrical and Computer Engineering, 2002. IEEE CCECE 2002. Canadian Conference on, vol.2, pp. 1105-1110
[15] Syeda-Mahmood T, Beymer D, Wang F 2007 Shape-Based Matching of ECG Recordings Engineering in Medicine and Biology Society, 2007. EMBS 2007. 29th Annual International Conference of the IEEE, pp.2012-2018
[16] Tuzcu V, Nas S 2005 Dynamic Time Warping as a Novel Tool in Pattern Recognition of ECG Changes in Heart Rhythm Disturbances Systems, Man and Cybernetics, 2005 IEEE International Conference on , vol.1, pp. 182- 186
[17] Aach J, Church G M 2001 Aligning Gene Expression Time Series with Time Warping Algorithms Bioinformatics, 17(6), pp. 495-508
[18] Hermans F, Tsiporkova E 2007 Merging Microarray Cell Synchronization Experiments Through Curve Alignment Bioinformatics, 23(2), pp. 64-70
[19] Faundez-Zanuy M 2007 On-Line Signature Recognition Based on VQ-DTW Pattern Recognition, 40(3), pp. 981-992
[20] Rath T M, Manmatha R 2003 Word Image Matching Using Dynamic Time Warping. Computer Vision and Pattern Recognition, 2003. Proceedings. 2003 IEEE Computer Society Conference on , vol.2, pp. 521-527
[21] Gollmer K, Posten C 1996 Supervision of Bioprocesses Using a Dynamic Time Warping Algorithm Control Engineering Practice, 4(9), pp. 1287-1295
[22] Senin P 2008 Dynamic Time Warping Algorithm Review Information and Computer Science Department University of Hawaii at Manoa Honolulu, USA
[23] Zhen D, Alibarbar A, Zhou X, Gu F S, and Ball A D 2011 Electrical Motor Current Signal Analysis using a Dynamic Time Warping Method for Fault Diagnosis J. Phys.: Conf. Ser. 305 012093
[24] Henniger O and Muller S 2007 Effects of time normalization on the accuracy of dynamic time warping In BTAS, 27–29, IEEE
[25] Xie Y and BryanWiltgen 2010 Adaptive Feature Based Dynamic Time Warping In IJCSNS International Journal of Computer Science and Network Security, vol. 10, no.1, pp. 264-273

[26] Schoen R R, Habetler T G, Kamran F, Bartfield R G 1995 Motor bearing damage detection using stator current monitoring Industry Applications, IEEE Transactions on , vol.31, no.6, pp.1274-1279
[27] Bellini A, Filippetti F, Franceschini G, Tassoni C, Kliman G B 2001 Quantitative evaluation of induction motor broken bars by means of electrical signature analysis Industry Applications, IEEE Transactions on, vol.37, no.5, pp.1248-1255
[28] Filippetti F, Franceschini G and Tassoni C 1998 AI techniques in induction machines diagnosis including the speed ripple effect Industry Applications, IEEE Transactions on, vol.34, no.1, pp.98-108
[29] Kruskal J B and Liberman M 1983 The symmetric time-warping problem: from continuous to discrete. Time warps, string edits, and macromolecules: the theory and practice of sequence comparison. CSLI Publications, Stanford, pp. 125-161